

Optically-controlled manipulation of live cells using optoelectronic tweezers

Aaron T. Ohta, Pei-Yu Chiou, Ming C. Wu

Berkeley Sensor & Actuator Center / Dept. of Electrical Engineering & Computer Sciences
Univ. of California, Berkeley, Berkeley, CA, USA 94720

ABSTRACT

Optoelectronic tweezers (OET) provides a non-invasive, low-power, optical manipulation tool for trapping, transporting, and separating microparticles, cells, and other bioparticles. The OET device uses a photosensitive layer to form "virtual electrodes" upon exposure to light, creating non-uniformities in an applied electric field. The electric field gives rise to a force known as dielectrophoresis: microparticles move as a result of the non-uniformities in the electric field imparting unequal forces on the induced dipoles of the particles. These virtual electrodes can be actuated with low optical intensities, enabling the use of incoherent light sources and direct imaging techniques to create optical manipulation patterns in real-time. In this paper, we demonstrate OET operation on live cells, including the trapping and manipulation of red and white blood cells, and the automated collection of HeLa cells. Automated size-based sorting is performed on a mixture of 15- and 20- μm -diameter polystyrene beads, and dielectric property-based separation is used to differentiate between live and dead white blood cells.

Keywords: Optoelectronic tweezers, optically-induced dielectrophoresis, dielectrophoresis, optical manipulation

1. INTRODUCTION

Biology at the individual cell level promises to provide researchers with a deeper understanding of cellular behavior, signaling, and other mechanisms. Thus, the ability to manipulate individual cells is extremely attractive for these researchers. One technology that is currently used for cell manipulation is optical tweezers, which uses the gradient force of a highly-focused laser to trap cells and other microparticles. Developed by Ashkin, et al.^{1,2}, this technology has been used for a wide variety of biological experiments³⁻⁷. The functionality of optical tweezers has been increased with the development of holographic optical tweezers⁸, optical vortices⁹, optical lattices¹⁰, Bessel beam traps¹¹, and other variations on the optical landscape.

As optical tweezers is a non-contact method of cell manipulation, it has been well-received by the biological community. However, optical tweezers does have some disadvantages. High optical intensities (approximately 0.1 to 1 MW/cm²) are required to produce sufficient trapping forces. These intensities are high enough to affect cellular metabolism¹², or even kill the cells under manipulation³. In addition, the creation of an optical tweezers trap requires a highly-focused laser. Typically, high numerical aperture objective lenses are used, limiting the area over which the optical trap can be formed. An alternative optical trapping method, which relies on the optical force produced by the evanescent wave of a beam undergoing total internal reflection, overcomes the effective area limitation, although high-power lasers are still utilized¹³.

Another type of cellular manipulation technology uses the gradient force of a non-uniform electric field to produce a force. This force, known as dielectrophoresis (DEP), was first observed by Pohl¹⁴. Microfabrication techniques have been used to create metal electrode patterns that provide non-uniform fields suitable for cellular manipulation^{15, 16}. However, unlike optical tweezers, it is difficult to alter the potential landscape in these microfabricated devices. Spatially-varying electric fields can be produced by applying alternating phases to electrode arrays, in what is known as traveling-wave dielectrophoresis¹⁷. However, it is difficult to manipulate a particular cell of interest using either conventional dielectrophoresis or traveling-wave dielectrophoresis. To address these shortcomings, an active device was demonstrated that creates dynamic DEP traps on a complementary metal oxide semiconductor- (CMOS) based circuit

platform¹⁸. However, the electrode pitch (20 μm) limits the resolution of this device. In addition, electrode addressing becomes an issue for large arrays.

Our group has developed a tool that addresses the drawbacks of current cellular manipulation technology. Optoelectronic tweezers (OET) provides a non-invasive, low-power, optical manipulation tool for trapping, transporting, and sorting microparticles, cells, and other bioparticles. The OET device uses a photosensitive material to enable optically-induced dielectrophoresis. The optical pattern is used to control the electric field within the device, and does not act upon the cells directly; thus, OET can be actuated with optical intensities 100,000 times less than optical tweezers. This low power requirement allows the use of direct imaging and incoherent light to create optical manipulation patterns in real-time. We have demonstrated microparticle trapping using a variety of incoherent light sources, including a single LED. Complex manipulation patterns can be easily produced using spatial light modulators. The resolution of these patterns is diffraction-limited, allowing the precise manipulation of live single cells. In addition, as there is no requirement for highly-focused light, the optical patterns can be projected over an area that is 500 times larger than that of a typical optical tweezers setup.

Optoelectronic tweezers can be easily used to trap and transport microparticles and cells. This was first demonstrated by using a focused 0.8-mW HeNe laser to move 25- μm polystyrene beads¹⁹ and *E. coli* bacteria²⁰. Subsequently, OET actuation was obtained by focusing the output of a computer projector²¹, allowing the creation of more complex trapping patterns²². Another group has used a similar device and setup to trap yeast cells²³. We have also trapped a large number of microparticles, demonstrating the massively parallel manipulation capabilities of OET, as well as the ease of optical addressing²⁴.

In addition to microparticle and cell trapping, OET is capable of separating heterogeneous particle populations, based on particle size or on the dielectric property differences among the particles. Size-based sorting of polystyrene beads was previously demonstrated using an optical sorter²⁴.

In this paper, we will describe the operation of OET on live cells, including the trapping and manipulation of red and white blood cells, and the automated collection of HeLa cells. We also present the separation of heterogeneous samples using OET. Image analysis techniques are used to control the separation of a mixed sample of 15- and 20- μm -diameter polystyrene beads. We also perform the selective concentration of live human B cells from a mixture of live and dead cells.

2. OPTOELECTRONIC TWEEZERS DEVICE

Optoelectronic tweezers creates optically-induced dielectrophoresis by creating virtual electrodes on a photosensitive surface. The optical setup and device structure of OET is shown in Figure 1. The OET device uses two electrodes: an upper transparent electrode consisting of a 100-nm-thick indium-tin-oxide (ITO) layer on a glass substrate, and a lower photosensitive electrode. The photosensitive electrode consists of a glass substrate, a 100-nm-thick ITO layer for electrical bias, a thin (50 nm) highly-doped hydrogenated amorphous silicon (a-Si:H) layer, and an intrinsic, 1- μm -thick photoconductive layer of a-Si:H. Spacers are placed between the electrodes to form a chamber that is 100 μm in height. Aqueous solutions containing cells or microparticles are introduced into this chamber. An ac voltage is placed across the two OET electrodes to provide the electric field necessary for operation.

Optical patterns are focused onto the photosensitive OET electrode, typically by a 10x microscope objective (N.A. = 0.3). The optical patterns can be created by intensity modulators, such as the digital micromirror device (DMD, Texas Instruments), or by phase modulators, such as liquid-crystal modulators produced by Hamamatsu (PAL-SLM). The optical source OET actuation is flexible, as low light intensities are sufficient, and coherent light is not required. The types of light sources used in the experiments described in this paper include a 0.8-mW HeNe laser, a 100-W halogen lamp, a 625-nm LED (Luxeon Star/O), and a 10-mW, 635-nm diode laser (used with the PAL-SLM, with a 5x beam expander).

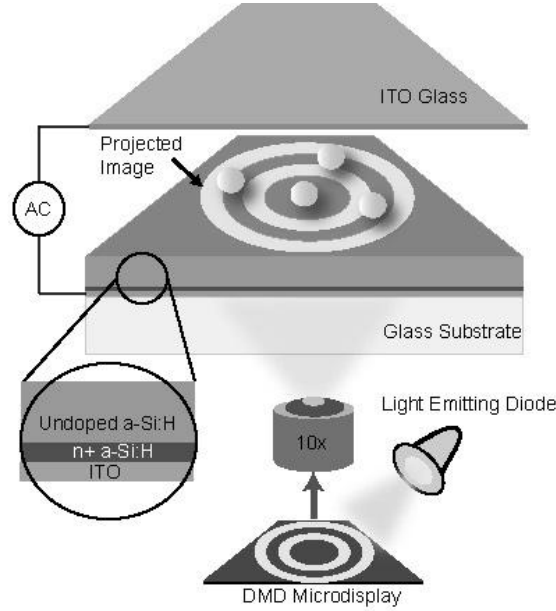


Fig. 1. Optical setup and device structure of optoelectronic tweezers. The device consists of an upper transparent electrode of ITO-coated glass, and a lower photosensitive electrode, with a photoconductive layer of hydrogenated amorphous silicon (a-Si:H). Optical manipulation patterns are generated and focused onto the photosensitive electrode, enabling the actuation of microparticles and cells.

The photoconductive amorphous silicon layer enables the creation of virtual electrodes in the OET device. The a-Si:H layer has a dark conductivity of 10^{-8} S/m, while the typical liquid conductivity is 10^{-2} S/m. Thus, most of the applied ac voltage is dropped across the a-Si:H. However, once illuminated by the projected optical pattern, the conductivity of the a-Si:H layer increases by several orders of magnitude, to approximately 10^{-3} S/m. This photoconductivity is sufficient to lower the impedance of the illuminated a-Si:H below that of the liquid layer, resulting in a significant voltage drop across the liquid layer in the illuminated areas of the OET device. This creates a non-uniform electric field in the liquid layer, which imparts a dielectrophoretic force on the microparticles or cells that are present. The important impedances present in the OET device are shown in Figure 2. The dark impedance of the a-Si:H (a-Si:H off) must be greater than the liquid impedance. In addition, the illuminated impedance of the a-Si:H (a-Si:H on) must be lower than the liquid impedance to ensure that the virtual electrode is switched on. Two liquid conductivities are plotted here, 10 mS/m and 50 mS/m.

The force that is induced in the OET device is dielectrophoresis, the force produced on an induced dipole in the presence of a non-uniform electric field¹⁴. Thus, conventional dielectrophoresis theory can be used to describe the OET force, which is given by²⁵

$$F_{OET} = F_{DEP} = 2\pi r^3 \epsilon_m \operatorname{Re}[K(\omega)] \nabla E_{rms}^2 \quad (1)$$

for spherical particles. In this equation, r is the particle radius, ϵ_m is the permittivity of the medium surrounding the particle, E_{rms} is the root-mean-square electric field strength, and $\operatorname{Re}[K(\omega)]$ is the real part of the Clausius-Mossotti factor, given by²⁵

$$K(\omega) = \frac{\epsilon_p^* - \epsilon_m^*}{\epsilon_p^* + 2\epsilon_m^*}, \epsilon_p^* = \epsilon_p - j \frac{\sigma_p}{\omega}, \epsilon_m^* = \epsilon_m - j \frac{\sigma_m}{\omega} \quad (2)$$

where ϵ is the permittivity of the particle or medium, σ is the conductivity of the particle or medium, and ω is the angular frequency of the electric field. The magnitude of $\operatorname{Re}[K(\omega)]$ varies with frequency, resulting in a frequency-

dependence of the dielectrophoretic force (Fig. 3a). Positive values of $\text{Re}[K(\omega)]$ result in particle attraction to electric field maxima (positive DEP, also referred to as positive OET). For negative values of $\text{Re}[K(\omega)]$, particles are repelled from field maxima (negative DEP, also referred to as negative OET). Applying an ac electric field thus allows the tuning of the type of DEP force induced on a particle, as well as negating any electrophoretic effects, or particle movement due to its surface charge.

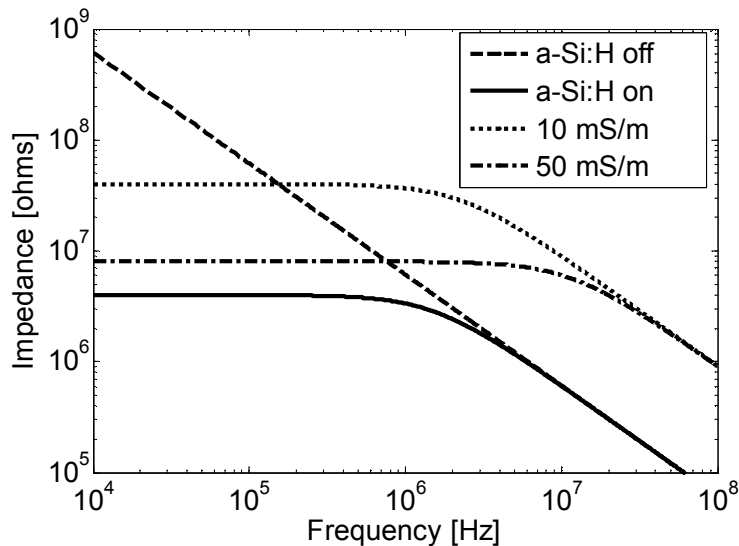


Fig. 2. Key impedances in the OET device. The dark impedance of the hydrogenated amorphous silicon is shown as “a-Si:H off,” while the illuminated impedance is “a-Si:H on.” Two liquid conductivities are plotted, 10 mS/m and 50 mS/m.

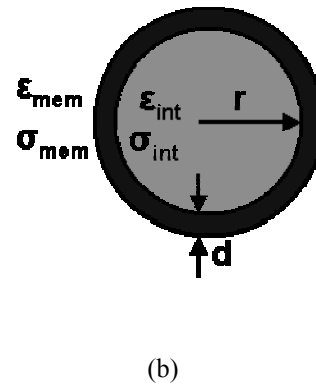
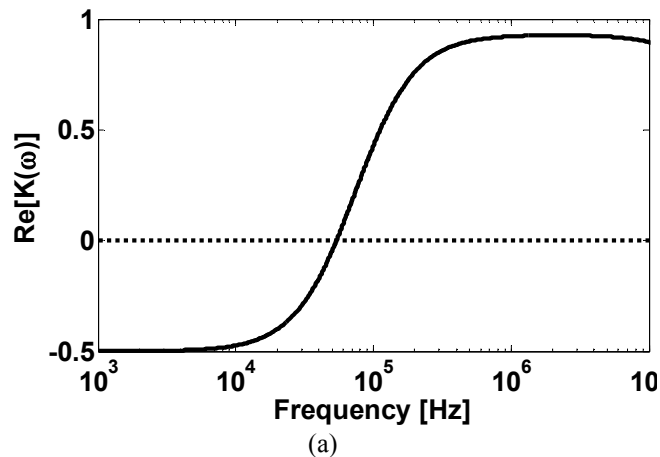


Fig. 3. (a) Real part of the Clausius-Mossotti factor as a function of frequency for human B cells in a 10 mS/m aqueous solution. Positive DEP occurs for $\text{Re}[K(\omega)] > 0$, and negative DEP for $\text{Re}[K(\omega)] < 0$. The cell parameters used for this simulation are from ref. ²⁶. (b) The single-shell model for mammalian cells. The Clausius-Mossotti factor can be determined from the following parameters: the permittivity and conductivity of the cell membrane and interior, the size of the cell interior, and the thickness of the cell membrane.

A single-shell model is typically used to determine the frequency-dependent Clausius-Mossotti factor for mammalian cells (Fig. 3b). The permittivity and conductivity of the cell membrane and interior are used to determine an effective complex permittivity that is used in Eq. 2. This effective permittivity is given by²⁷

$$\epsilon_p^* = C_{mem}^* \frac{3r\epsilon_{int}^*}{3\epsilon_{int}^* + 3C_{mem}^*r}, \quad (3)$$

assuming that the thickness of the cell membrane, d , is much less than the radius of the cell interior, r . The membrane capacitance, C_{mem}^* , is given by²⁷

$$C_{mem}^* = \frac{\epsilon_{mem}}{d} - \frac{j\sigma_{mem}}{d}. \quad (4)$$

Many cell types are uniquely distinguishable by the real part of the Clausius-Mossotti factor. This enables the separation of different cell types using DEP force^{27, 28}.

3. EXPERIMENTAL RESULTS

3.1 Microparticle / cell trapping and spatial patterning

The trapping of bovine red blood cells was achieved via optoelectronic tweezers. For this experiment, the optical source consisted of a 0.8-mW HeNe laser ($\lambda = 633$ nm). A spatial light modulator was not used in the setup; instead, a 10x objective lens was used to reduce the laser beam size to approximately 20 μm in diameter. Cell solutions were prepared from bovine serum. The red blood cells were isolated and suspended in an isotonic solution (8.5% sucrose, 0.3% dextrose) at concentrations ranging from approximately 1×10^6 to 1×10^7 cells/mL. Approximately 5 μL of this solution was introduced into the OET device.

A positive OET response was observed at an applied ac bias of 3 Vpp at 200 kHz, attracting the red blood cells towards the laser spot at velocities of up to 9 $\mu\text{m}/\text{s}$ (Fig. 4). Initially, the laser is on (Fig. 4a), but no electric field is applied. An ac bias is then applied to the OET device, producing OET force, which attracts the blood cells to the illuminated area (Fig. 4b). It was also observed that the cells align vertically along the electric field lines (Fig. 4b). When the laser is turned off, the concentrated cells remain in the trap area (Fig. 4c). After the applied voltage is switched off, the concentrated red blood cells began to slowly pulsate, migrating away from the trap area (Fig. 4d), implying that they remain alive and viable.

In order to achieve automated cell trapping, OET was integrated with an image-analysis feedback control system (Fig. 5a). In this system, the microscope image is analyzed by a custom-built code written for the Processing open source software (processing.org). The software scans the entire microscope image, identifying the locations of the cells within the field-of-view. This information is used to generate optical patterns near the target cells. The optical pattern information is projected onto the OET device via the spatial light modulator. The light source is a 10-mW, 635-nm diode laser, expanded by 5 times. The microscope stage is used to raster the OET device across the projected optical manipulation area, allowing separation to occur over the entire OET device area (Fig. 5b).

Automated cell trapping was achieved using HeLa cells suspended in an isotonic solution, at a concentration of approximately 5×10^5 cells/mL. In this experiment, the microscope stage that carries the OET device is moving, as well as the optical pattern. In Figure 6, the microscope stage is moving from the left to the right at a constant speed of 5 $\mu\text{m}/\text{s}$. The HeLa cells enter the active manipulation area from the left of the screen, and are recognized by the image analysis software. An optical pattern is created just below the cells, in the $-y$ direction. The cells experience a positive OET response at an ac frequency of 100 kHz, and are pulled towards to the bottom of the screen ($y = 0$). The optical trapping pattern is switched off once the cells reach the bottom of the screen. The trajectories of 10 cells (Fig. 6c) are linear, showing that the cells experience a constant DEP force across the active optical manipulation area.

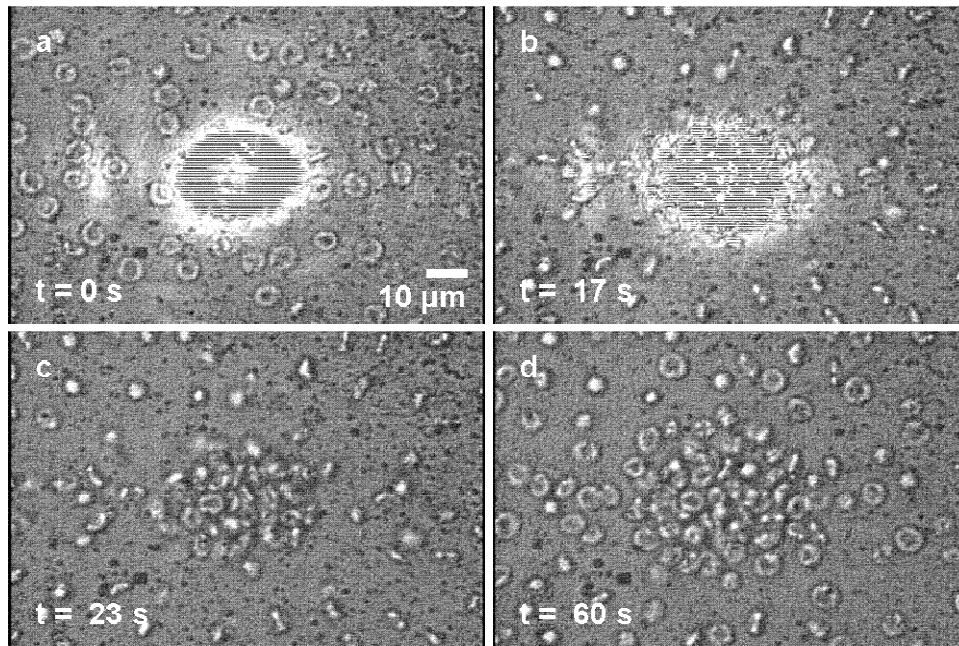


Fig. 4. Concentration of bovine red blood cells using OET. (a) Prior to applying an electric field, the blood cells are not attracted to the laser spot. (b) The applied voltage of 3 Vpp at 200 kHz is switched on. The red blood cells align vertically with the electric field and are attracted to the laser spot. (c) The laser and applied voltage are switched off. Red blood cells are clearly shown to be concentrated in the area of the laser spot. (d) The concentrated cells slowly diffuse out of the concentrated area.

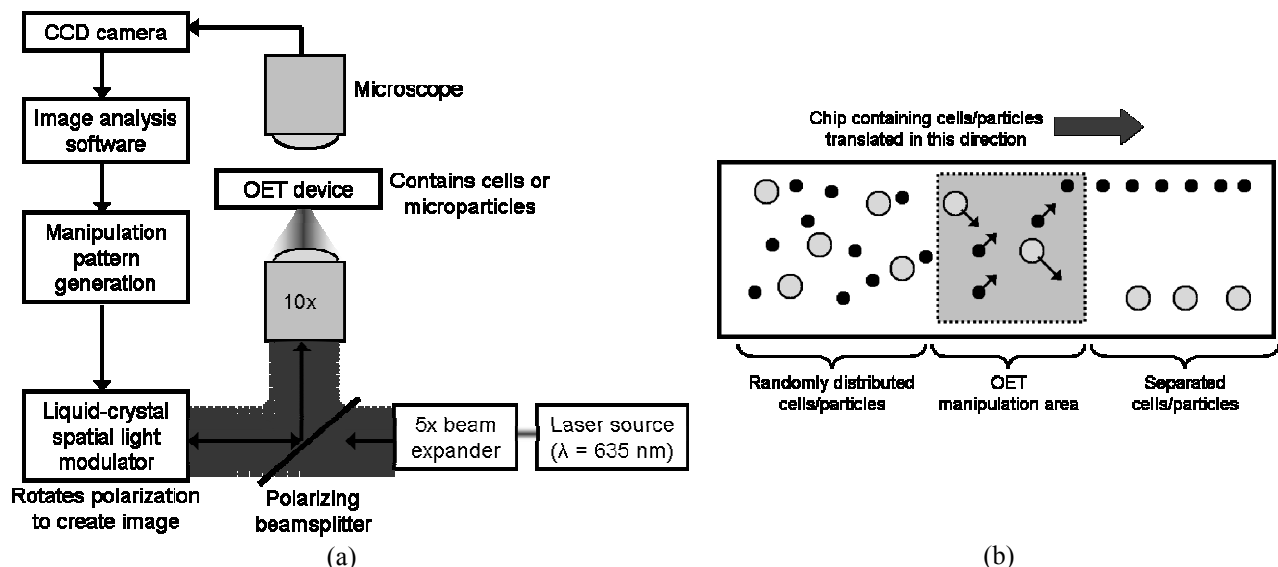


Fig. 5. (a) Image analysis system. The CCD camera captures the microscope image, which is analyzed and used to generate optical manipulation patterns for display by the spatial light modulator. (b) To achieve particle separation across the entire device, the stage is rastered across the projected area of the optical manipulation pattern.

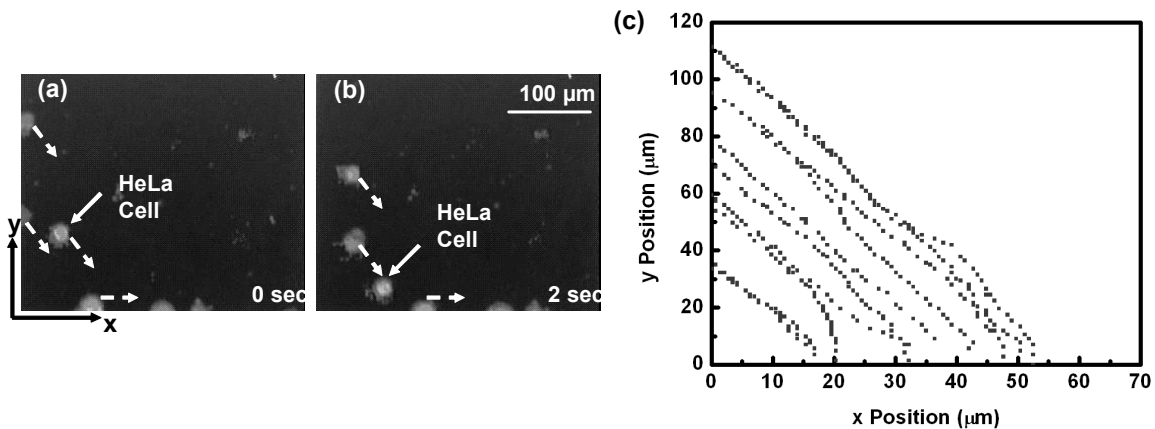


Fig. 6. (a, b) HeLa cells are concentrated towards the bottom of the images ($y = 0$). (c) Trajectories of 10 HeLa cells as they enter the active area from the left side of the image ($x = 0$).

The use of an incoherent light source and direct image patterning increases the flexibility and functionalities of OET. A spatial light modulator can pattern any arbitrary image to be projected onto the photoconductive surface, creating the corresponding virtual electrodes on the OET device. Complex, reconfigurable manipulation patterns can thus be created by simple software programming. This technique is demonstrated in the arrangement of human B cells into a complex pattern.

A 100-W halogen lamp was used as the incoherent optical source. The optical pattern was created using the Texas Instruments digital micromirror device (DMD). The DMD is a 1024 x 768 array of individually-addressable micromirrors, each of which is 13.68 μm x 13.68 μm. The images displayed on the DMD are controlled via a computer. The prepared cell solutions consisted of human white blood cells (B-lymphocytes), suspended in an isotonic solution at a concentration of approximately 5×10^5 cells/mL. Approximately 5 μL of this solution was introduced into the OET device.

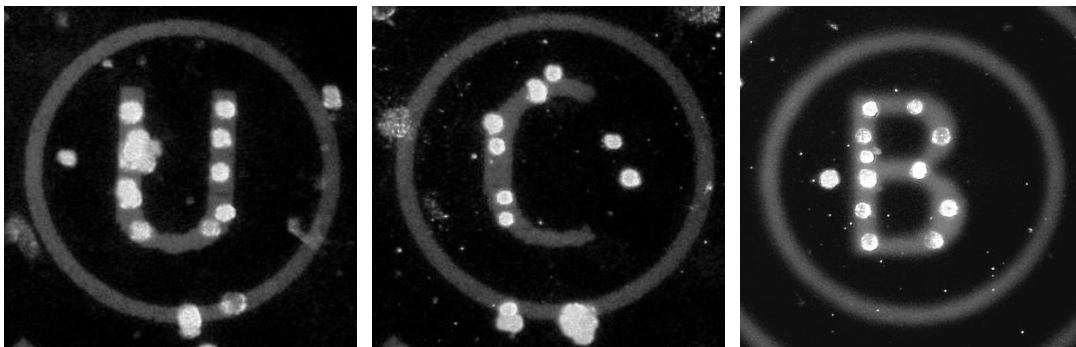


Fig. 7. Patterning of human white blood cells. Cells are attracted to the illuminated characters by positive OET. The ring is part of a concentric pattern that is used to concentrate the B cells towards the characters. Additional cells along the ring are moving in towards the characters.

The B cells can be manipulated into an arbitrary pattern. Here, we chose to assemble the cells into the shape of “U”, “C”, and “B” characters (for Univ. of Calif., Berkeley). At an applied bias of 14 Vpp at a frequency of 100 kHz, the white blood cells exhibit positive OET behavior. A shrinking concentric ring pattern is used to concentrate the cells towards the character image at velocities of approximately 9 μm/s (Fig. 7). Cells are attracted to each concentric ring. As the rings shrink, the cells are transported towards the center of the concentric rings, where the character image is projected. The cells then become trapped by the static character pattern. A few cells are not attracted to the character patterns (cells to the left of the “U” and the “B”, cell to the right of the “C”). These cells do not experience a positive

OET force at this applied frequency; instead, they have a negative OET response. It is likely that these cells are dead (see Section 3.2 for a more detailed discussion).

3.2 Microparticle and cell separation

The same experimental setup as described for the automated HeLa cell trapping experiment is used to provide image analysis-driven size-based separation of polystyrene beads. A mixture of 15- and 20- μm -diameter beads are suspended in a 10 mS/m KCl solution, and introduced into the OET device. The microscope stage is translated in the $+y$ direction at a velocity of 5 $\mu\text{m/s}$ (Fig. 8). The image analysis software recognizes the position and size of each particle. The appropriate optical patterns are then generated. For this experiment, the software was programmed to move the 20- μm beads to the left ($-x$ direction), and the 15- μm beads to the right ($+x$ direction). As the beads have a negative OET response, the optical pattern is created on the opposite side of the bead from the desired translation direction. The beads are then pushed in the desired direction. The particle trajectories for the two different sized populations were recorded, and are shown in Figure 8c.

In our current system, the throughput is limited by the refreshing rate of the Hamamatsu PAL-SLM, which is 5 frames per second. Moving the stage at a speed greater than 15 $\mu\text{m/s}$ introduces a time delay in the optical pattern projection. The densest particle concentration that has been successfully demonstrated in this system is 1600 beads/ mm^2 , corresponding to a sorting throughput of 120 beads/min in the active area.

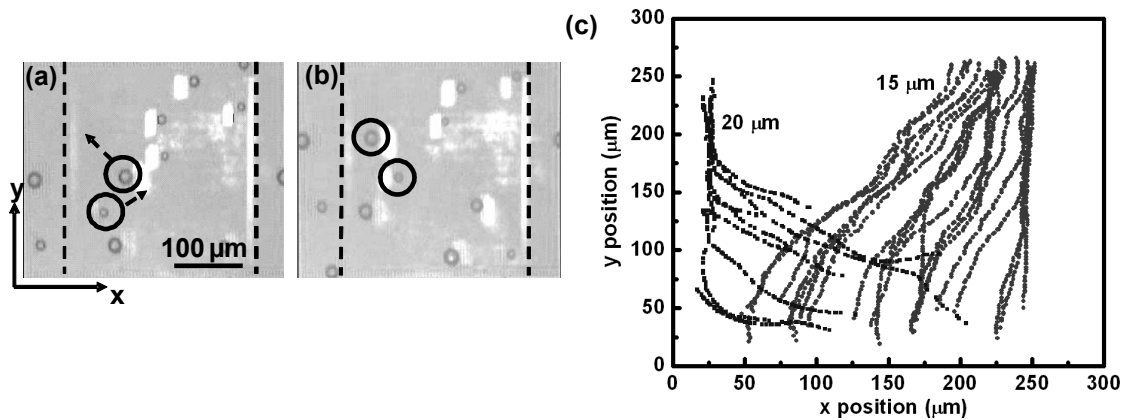


Fig. 8. (a, b) Continuous particle sorting on 15- and 20- μm -diameter polystyrene beads. The dashed bars show the position of the optical guiding bars. (c) Trajectories of the beads as they enter the active area from the bottom of the image ($y = 0$).

In addition to size-based separation, microparticles and cells can be separated based on dielectric property differences. This property is useful for cellular manipulation, in which heterogeneous mixtures of cells are common. Dielectric property differences can also be used to separate between cells of the same type, such as live and dead cells. In a live cell, the semi-permeable phospholipid membrane allows the cell to maintain an ion differential between the cell interior and the surrounding medium. If the cell suspension media consists of a low-conductivity isotonic buffer, as is the case for OET experiments, the cell will have an internal conductivity greater than the liquid (Fig. 9a). However, once the cell dies, the membrane becomes permeable to ions. The ion differential is no longer maintained, and the conductivity of the cell interior becomes the same as the surrounding liquid. This means that the Clausius-Mossotti factor is different for live and dead cells. The real part of the Clausius-Mossotti factor is calculated and plotted in Figure 9b. The simulated cell type is a human B cell. To determine the Clausius-Mossotti factor of dead B cells, it is assumed that the internal permittivity and conductivity of the cell is equal to that of the surrounding media, while all other parameters remain constant. The simulated results predict that for applied frequencies greater than approximately 60 kHz, live B cells will experience a positive OET force, while dead B cells will experience a negative OET force.

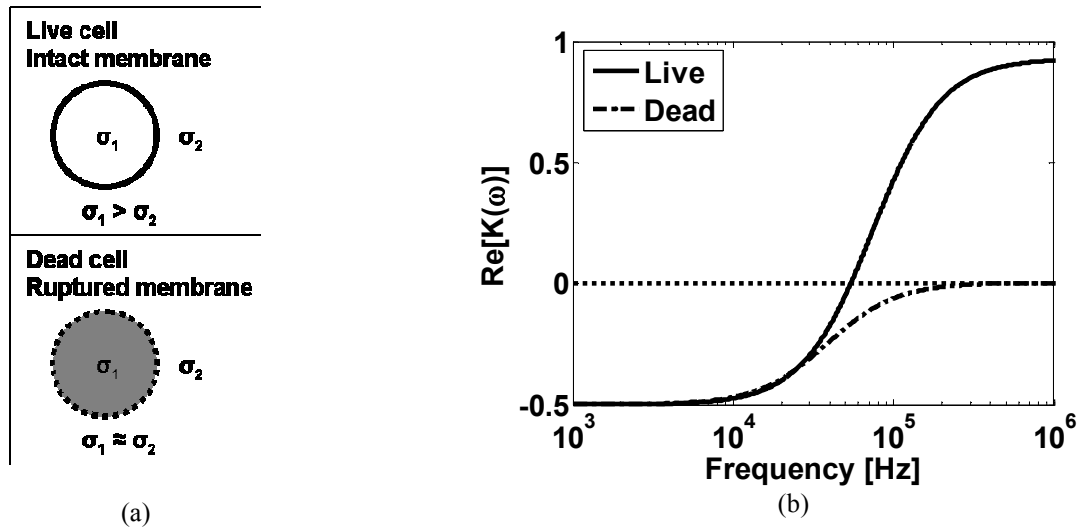


Fig. 9. (a) Live cells maintain an ion differential between their high-conductivity interior and the low-conductivity liquid. Dead cells lose this ability. (b) Real part of the Clausius-Mossotti factor for live and dead B cells.

The difference in DEP response between live and dead B cells is used to selectively concentrate live B cells at an applied frequency of 120 kHz. The selective collection pattern is a series of broken concentric rings (Fig. 10). The pattern is created using the DMD, and illumination is provided by a 100-W halogen lamp. As the concentric rings shrink, the live cells are focused to the center of the pattern by positive OET. In contrast, the dead cells experience negative OET, and slip through the gaps in the ring patterns. The B cells are suspended in isotonic solution, with 0.4% Trypan blue dye. The Trypan blue dye identifies live and dead cells; live cells exclude the dye, and appear clear. The dead cells, which have a permeable membrane, absorb the dye, and appear dark. The experiment is performed immediately after the addition of the Trypan blue dye, as the dye is toxic, and will increase the amount of dead cells in the sample.

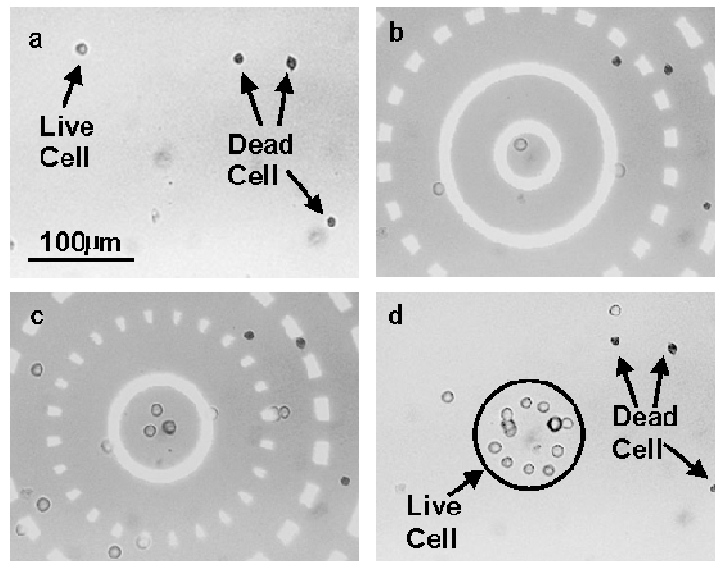


Fig. 10. Selective concentration of live B cells from dead cells. (a) The initial positions of live (clear) and dead (dark) B cells. (b, c) A broken concentric ring pattern is used to transport the live cells to the center of the field of view while leaving the dead cells behind. (d) The live cells have been concentrated to the central region of the optical pattern.

4. CONCLUSION

Optoelectronic tweezers provides a potent tool for single-cell manipulation. OET offers non-invasive, flexible individual cell manipulation over a large area. Many discrete functions can be integrated on a single device, simply by altering the optical manipulation pattern. We have demonstrated the trapping of bovine red blood cells at up to 9 $\mu\text{m/s}$, the patterning of human B cells, and the automated trapping of HeLa cells. In addition, the separation of heterogeneous particle samples were performed, including image analysis-driven size-based particle separation at up to 120 particles/min., and the selective concentration of live cells from dead cells. We believe that OET will become an important tool in single-cell research.

ACKNOWLEDGMENTS

The authors would like to thank the following research groups for their assistance with the cell experiments presented here: James C. Liao's group (UCLA), Edward R.B. McCabe's group (UCLA), Ren Sun's group (UCLA), and Luke Lee's group (UC Berkeley). We would also like to thank UC Berkeley's Tissue Culture Facility for providing HeLa cells. This project is supported by the Center for Cell Mimetic Space Exploration (CMISE), a NASA University Research, Engineering and Technology Institute (URETI), under award number #NCC 2-1364. A. Ohta is funded by an NSF Graduate Research Fellowship. P. Y. Chiou is partially funded by a UC GREAT fellowship.

REFERENCES

- [1] A. Ashkin, "Acceleration and trapping of particles by radiation pressure," *Physical Review Letters* **24**, 156-9, 1970.
- [2] A. Ashkin, J. M. Dziedzic, J. E. Bjorkholm, and S. Chu, "Observation of a single-beam gradient force optical trap for dielectric particles," *Optics Letters* **11**, 288-90, 1986.
- [3] A. Ashkin and J. M. Dziedzic, "Optical trapping and manipulation of viruses and bacteria," *Science* **235**, 1517-20, 1987.
- [4] A. Ashkin, J. M. Dziedzic, and T. Yamane, "Optical trapping and manipulation of single cells using infrared laser beams," *Nature* **330**, 769-71, 1987.
- [5] S. Chu, "Laser manipulation of atoms and particles," *Science* **253**, 861-6, 1991.
- [6] T. Kaneta, N. Mishima, and T. Imasaka, "Determination of motility forces of bovine sperm cells using an "optical funnel", " *Analytical Chemistry* **72**, 2414-2417, 2000.
- [7] B. Maier, I. Chen, D. Dubnau, and M. P. Sheetz, "DNA transport into *Bacillus subtilis* requires proton motive force to generate large molecular forces," *Nat. Struct. Mol. Biol.* **11**, 643-649, 2004.
- [8] J. E. Curtis, B. A. Koss, and D. G. Grier, "Dynamic holographic optical tweezers," *Optics Communications* **207**, 169-75, 2002.
- [9] J. E. Curtis and D. G. Grier, "Structure of optical vortices," *Physical Review Letters* **90**, 133901/1-4, 2003.
- [10] M. P. MacDonald, G. C. Spalding, and K. Dholakia, "Microfluidic sorting in an optical lattice," *Nature* **426**, 421-4, 2003.
- [11] L. Paterson, E. Papagiakoumou, G. Milne, V. Garces-Chavez, S. A. Tatarkova, W. Sibbett, F. J. Gunn-Moore, P. E. Bryant, A. C. Riches, and K. Dholakia, "Light-induced cell separation in a tailored optical landscape," *Applied Physics Letters* **87**, 2005.
- [12] K. C. Neuman, E. H. Chadd, G. F. Liou, K. Bergman, and S. M. Block, "Characterization of photodamage to *Escherichia coli* in optical traps," *Biophysical Journal* **77**, 2856-2863, 1999.
- [13] P. J. Reece, V. Garces-Chavez, and K. Dholakia, "Near-field optical micromanipulation with cavity enhanced evanescent waves," *Applied Physics Letters* **88**, 2006.
- [14] H. A. Pohl, *Dielectrophoresis*. Cambridge: Cambridge University Press, 1978.
- [15] P. R. C. Gascoyne, J. V. Vykoukal, J. A. Schwartz, T. J. Anderson, D. M. Vykoukal, K. W. Current, C. McConaghy, F. F. Becker, and C. Andrews, "Dielectrophoresis-based programmable fluidic processors," *Lab On A Chip* **4**, 299-309, 2004.

- [16] S. N. Higginbotham and D. R. Sweatman, "Fabrication methods, operation, and measurement of electrokinetic fluid manipulation devices," *Proc. of SPIE-Int. Soc. Opt. Eng. Proceedings of Spie - the International Society for Optical Engineering*, vol.5275, no.1, 2004, pp.335-44. USA., 2004.
- [17] R. Pethig, M. S. Talary, and R. S. Lee, "Enhancing traveling-wave dielectrophoresis with signal superposition," *IEEE Engineering In Medicine And Biology Magazine* **22**, 43-50, 2003.
- [18] N. Manaresi, A. Romani, G. Medoro, L. Altomare, A. Leonardi, M. Tartagni, and R. Guerrieri, "A CMOS chip for individual cell manipulation and detection," *IEEE Journal of Solid-State Circuits* **38**, 2297-305, 2003.
- [19] P. Y. Chiou, Z. Chang, and M. C. Wu, "A Novel Optoelectronic Tweezer Using Light Induced Dielectrophoresis," *Proc. of IEEE/LEOS International Conference on Optical MEMS*, 8-9, Kona, Hawaii, USA, 2003.
- [20] P. Y. Chiou, W. Wong, J. C. Liao, and M. C. Wu, "Cell Addressing and Trapping Using Novel Optoelectronic Tweezers," *Proc. of 17th IEEE International Conference on Micro Electro Mechanical Systems (MEMS)*, 21-24, Maastricht, Netherlands, 2004.
- [21] A. T. Ohta, P. Y. Chiou, and M. C. Wu, "Dynamic DMD-driven optoelectronic tweezers for microscopic particle manipulation," *Proc. of Conference on Lasers and Electro-Optics (CLEO)*, 3, San Francisco, CA, 2004.
- [22] A. T. Ohta, P. Y. Chiou, and M. C. Wu, "Dynamic array manipulation of microscopic particles via optoelectronic tweezers," *Proc. of Solid State Sensor, Actuator and Microsystems Workshop (Hilton Head)*, 216-219, Hilton Head, SC, USA, 2004.
- [23] Y.-S. Lu, Y.-P. Huang, J. A. Yeh, C. Lee, and Y.-H. Chang, "Controllability of non-contact cell manipulation by image dielectrophoresis (iDEP)," *Optical and Quantum Electronics* **37**, 1385-95, 2005.
- [24] P. Y. Chiou, A. T. Ohta, and M. C. Wu, "Massively parallel manipulation of single cells and microparticles using optical images," *Nature* **436**, 370-372, 2005.
- [25] T. B. Jones, *Electromechanics of Particles*. Cambridge: Cambridge University Press, 1995.
- [26] J. Yang, Y. Huang, X. J. Wang, X. B. Wang, F. F. Becker, and P. R. C. Gascoyne, "Dielectric properties of human leukocyte subpopulations determined by electrorotation as a cell separation criterion," *Biophysical Journal* **76**, 3307-3314, 1999.
- [27] P. R. C. Gascoyne, W. Xiao-Bo, H. Ying, and F. F. Becker, "Dielectrophoretic separation of cancer cells from blood," *IEEE Transactions on Industry Applications* **33**, 670-8, 1997.
- [28] Y. Huang, J. M. Yang, P. J. Hopkins, S. Kassegne, M. Tirado, A. H. Forster, and H. Reese, "Separation of simulants of biological warfare agents from blood by a miniaturized dielectrophoresis device," *Biomedical Microdevices* **5**, 217-225, 2003.